Kinetics and Mechanism of HO_2 Uptake on Solid NaCl

R. G. Remorov,[†] Yu. M. Gershenzon,*[,†] L. T. Molina,[‡] and M. J. Molina[‡]

Institute of Chemical Physics, Russian Academy of Sciences, 4 Kosygin St., Moscow 117977, Russian Federation, and Departments of Earth, Atmospheric and Planetary Sciences and of Chemistry, Massachusetts Institute of Technology, Cambridge, Massachusetts 02139

Received: August 16, 2001; In Final Form: February 14, 2002

The interaction of HO_2 radicals with solid NaCl has been investigated. The uptake coefficient γ was measured using a coaxial reactor with a movable central rod covered with NaCl. The radicals were detected at low concentrations ($\sim 4 \times 10^{10}$ molecule/cm^3) by matrix isolation ESR and at high concentrations ($\sim 5 \times 10^{11}$ molecule/cm^3) by titration with NO followed by gas-phase EPR detection. In the temperature range from 243 to 295 K, the apparent activation energy of γ does not depend on the HO_2 concentration. The γ value measured on NaCl agrees well with our previous γ value for nonreactive uptake by NH_4NO_3 in this temperature range. Furthermore, in the temperature range from 331 to 335 K, the γ value decreases sharply at low HO_2 concentrations. A combined Eley−Rideal and Langmuir−Hinshelwood mechanism with reasonable parameter values can explain the observations; such a mechanism is also consistent with the observation of an inhibition effect of water vapor on the uptake coefficient. The conclusion is that, in the coastal troposphere, the heterogeneous loss of HO_2 is of comparable importance to the homogeneous loss, particularly in the evening, when the HO_2 concentration is low.

Introduction

The hydrogen-containing radicals OH and HO_2 (HO_x) are key species for the oxidation and transformation of pollutants in the troposphere. Changes in the HO_x concentration affect the balance of such ozone-active species as NO_x, ClO_x, and BrO_x. Moreover, HO_x radicals participate in the hydrogen cycle of tropospheric ozone destruction:

$$OH + O_3 \rightarrow HO_2 + O_2$$

$$HO_2 + O_3 \rightarrow OH + 2O_2$$

According to previous studies, both the sources and sinks of HO_2 radicals are determined by a number of gas-phase photochemical processes. The available laboratory data on the probabilities of the heterogeneous uptake of these radicals on surfaces that simulate atmospheric aerosol surfaces is scarce (see, e.g., Gershenzon et al.[1]) and suggests that the γ_{HO2} values are rather high ($\sim 0.01-0.1$). Atmospheric modeling calculations show that for such high values the heterogeneous uptake of HO_x (and especially HO_2) radicals on aerosol species has a significant effect on the gaseous composition of the troposphere.[2]

Recent studies have indicated that, besides hydroxyl radicals, atomic chlorine can also initiate the oxidation of volatile organic compounds (VOCs) in the marine boundary layer. The strongest support for this idea is provided by the direct detection of molecular chlorine at night and predawn in the coastal troposphere,[3] as well as by the observed morning consumption of natural hydrocarbons in the marine troposphere.[4] The atomic chlorine concentrations estimated from these and other results are $\sim 10^5$ molecule/cm^3. The rates of the reactions of chlorine atoms with most VOCs are 1−3 orders of magnitude higher than rates of the corresponding hydroxyl radical reactions. Therefore, the rates of initiation of VOC oxidation by chlorine atoms may be higher than that of the corresponding reaction with OH radicals at noon, when the OH concentration is maximum ([OH] = $(1-3) \times 10^6$ molecule/cm^3).

Laboratory studies have suggested several sources of the photochemically active chlorine compounds involving, for example, heterogeneous reactions of nitrogen oxides with sea salt aerosols, largely consisting of NaCl. However, the information available indicates that the heterogeneous reaction rates for these processes are not fast enough to generate the inferred high Cl-atom concentrations in the remote marine atmosphere,[4] where the concentration of nitrogen oxides is low.

In principle, the reaction of HO_2 radicals with NaCl can produce Cl_2 via the heterogeneous reaction

$$HO_2(g) + NaCl(s) = NaOH(s) + {}^1/_2(Cl_2 + O_2) \qquad \Delta H = -6 \text{ kcal/mol} \quad \text{(R1)}$$

where the indices g and s stand for gas and solid, respectively.

Another possible reaction of HO_2 with NaCl is the catalytic heterogeneous recombination (disproportionation)

$$HO_2(g) + NaCl(s) = {}^1/_2(H_2O_2 + O_2)(g) + NaCl(s) \quad \text{(R2)}$$

The uptake of HO_2 radicals on sea salt aerosols may cause a decrease in the HO_2 concentration, which in turn indirectly affects the concentrations of both OH and active chlorine and bromine compounds via the reactions

$$HO_2 + ClO \rightarrow HOCl + O_2 \quad \text{(R3)}$$

$$HO_2 + BrO \rightarrow HOBr + O_2 \quad \text{(R4)}$$

* To whom correspondence should be addressed. E-mail: gershenzon@center.chph.ras.ru.

[†] Russian Academy of Sciences.

[‡] Massachusetts Institute of Technology.

10.1021/jp013179o CCC: $22.00
Published on Web 04/04/2002

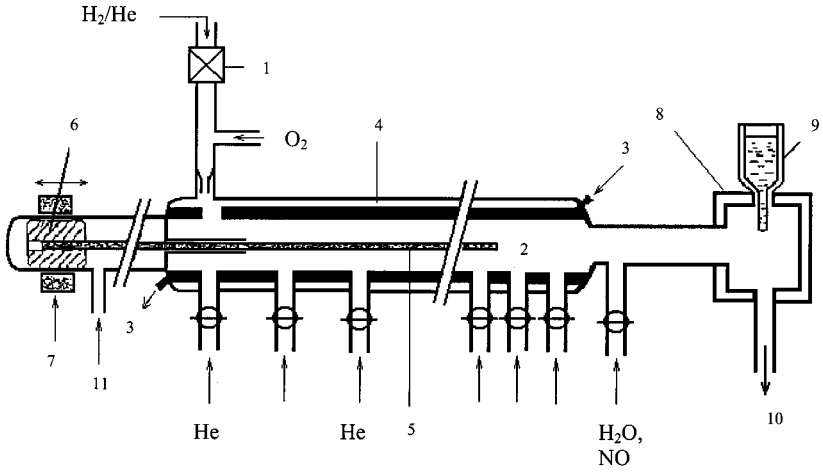

Figure 1. Schematic of the experimental apparatus for studying the heterogeneous uptake of radicals by EPR and MIESR. (1) High-frequency-discharge cavity, (2) reactor, (3) jacket with a thermostating liquid, (4) jacket for thermal insulation, (5) central moveable rod, (6 and 7) steel holder and magnet to move the rod, (8) EPR cavity, (9) Dewar flask with liquid nitrogen, (10) to pump, and (11) He flow to prevent back diffusion.

The main source of solid aerosol particles containing ~77 wt % of NaCl consists of liquid marine aerosol droplets generated under the action of sea waves and winds followed by water evaporation at a low humidity (<50%).[5] Continental dust may also contain NaCl. Woods et al.[6] estimated that the overall NaCl concentration in the stratospheric volcanic cloud particles of the El Chichon volcano (1982) was up to 7%.

The interaction of HO_2 radicals with solid NaCl surfaces has been investigated earlier: Antsupov[7] measured the probabilities of HO_2 uptake on solid NaCl surfaces at 300−365 K, and Gratpanche et al.[8] determined γ_{HO2} values at 243−293 K. Both groups found a negative activation energy for the γ value. Gershenzon et al.[9] showed that the γ value at room temperature is independent of the HO_2 concentration for values in the range from 4×10^9 to 3×10^{11} molecule/cm^3. The room temperature γ values listed in these three reports are in good agreement ($\sim 10^{-2}$). All three studies were carried out with flow systems operating at 1−3 Torr.

The data obtained in the previous studies do not provide sufficient information to establish the chemical mechanism of the process. An understanding of this mechanism is necessary to determine the γ value under realistic atmospheric conditions, that is, with HO_2 concentration lower than $(2-3) \times 10^8$ molecule/cm^3, which is much lower than that employed in the above measurements. Moreover, it is important to study the effect of water vapor on the γ value, which has not been investigated so far. Finally, the apparent negative activation energies of the uptake coefficient (~4.6 [7] and 7.5 kcal/mol[8]) appear too high.

The purpose of this work is to study the mechanism of HO_2 uptake on solid NaCl surfaces and, on this basis, to estimate the γ values under realistic atmospheric conditions. To do this, we studied in detail the temperature dependence of the HO_2 uptake probabilities with initial HO_2 concentrations of 4×10^{10} at 263−345 K and 5×10^{11} molecule/cm^3 at 243−295 K; we also investigated the effect of water vapor on the process.

Experimental Section

The experiments have been carried out by means of a new magnetic resonance installation for studying the uptake of polyatomic radicals on solid surfaces.[9] This technique is based on the matrix isolation of radicals trapped at liquid-nitrogen temperature and observation by electron spin resonance (ESR).

In laboratory experiments involving matrix isolation, the carrier gas and the radicals usually move directly to the cold surface, and the cold "finger" is placed in the center of the electron paramagnetic resonance (EPR) cavity.[10] This configuration restricts the carrier gas flux to ca. 10^{-5} mol/s.[11] Any larger flux would heat the finger, making the EPR spectrum unstable; therefore, the matrix isolation technique is not feasible under fast flow conditions.

Figure 1 presents a schematic of the experimental setup, which is a modification of the radical trapping technique employed earlier in our laboratory.[9,12] The fast flow coaxial reactor (2) is connected to the EPR cavity (8) via an inlet that is perpendicular to the EPR cavity axis. The carrier gas bypasses the cold finger (9) that is shifted 5−7 mm from the axis of the flow. This allows increasing the He carrier gas flow to 10^{-3} mole/s without any perceptible change in the radical trapping conditions. The gas flow velocity in the 2.1 cm diameter reactor is typically about 1500 cm/s at 1−3 Torr.

The high sensitivity of the matrix isolation technique ($\sim 10^8$ molecule/cm^3) persists when the radical delivery to the cold finger occurs by diffusion. On the other hand, this technique enables fast flow conditions and thus facilitates measurements of high rate chemical reactions involving polyatomic radicals.

The design shown in Figure 1 includes a high-pressure source of HO_2 produced by the $H + O_2 + M$ reaction. The H atoms originate from a microwave discharge of He (1) containing a very small amount of H_2. A small capillary separates the reactor from the high-pressure HO_2 source.

The sidearm inlets are used to measure the radical decay on the internal wall of the coaxial reactor. For this purpose, an additional flux of He carrier gas is passed through the different sidearm inlets; the "additional flux method" changes the contact time of the radicals with the cylinder wall enabling the determination of the uptake coefficient for the wall material.[13]

The uptake coefficient of HO_2 on halocarbon wax is 7.8×10^{-4} at 293 K. It slowly increases when the temperature falls to 243 K.[14] An additional He flow is added through inlet (11) to prevent the back diffusion of HO_2 in the reactor.

The efficiency of the matrix-isolation ESR method (MI ESR) can be improved if water vapor is added for radical stabilization through the inlet nearest to the EPR cavity. Figure 2 illustrates how the rate of HO_2 accumulation increases with the addition of water vapor. As seen in the figure, the background content of water vapor in the reactor is lower than 5×10^{12} molecule/cm^3. The experiments are carried out with water vapor added at $[H_2O] \sim 10^{14}$ molecule/cm^3.

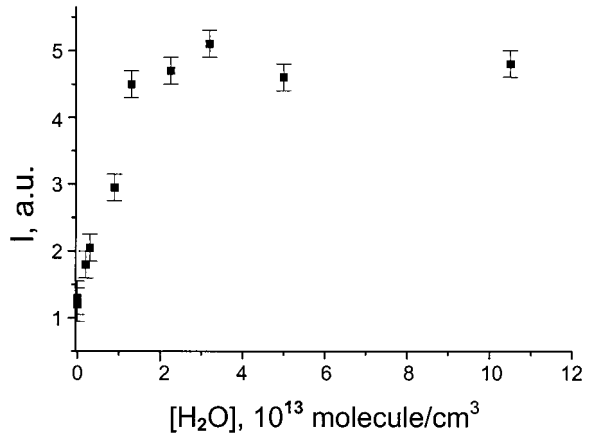

Figure 2. Rate of HO_2 accumulation as a function of water vapor concentration.

The 40 cm long central rod of the coaxial reactor (5) can be moved with help of an external magnet (6), as shown in Figure 1. This movement changes the interaction time of HO_2 with the rod. The experiments were carried out under two sets of conditions: (i) $[HO_2] = 4 \times 10^{10}$ molecule/cm^3, rod diameter 3.5 mm, $T = 263-345$ K, $p = 1$ Torr, and HO_2 radical detection with the MI ESR technique; and (ii) $[HO_2] = 5 \times 10^{11}$ molecule/cm^3, rod diameter 2.6 mm, $T = 243-295$ K, $p = 2.3$ Torr, and HO_2 radical detection by titration with NO followed by gas-phase EPR detection of OH. In this case, NO was added instead of water to the cavity inlet located closest to the EPR cavity.

The flow reactor is double jacketed: the temperature is maintained by pumping ethanol through the inner jacket by means of a MK-70 cryostat, and the outer jacket is under vacuum for thermal insulation.

Before coating with NaCl, the rod inserts were treated with HF for 1 min and then with potassium dichromate for 20 min and finally washed with distillated water. A saturated NaCl solution in distilled water was used for coating. The quartz rod was dipped into the solution at room temperature. After this, it was dried with a warm airflow at 40−70 °C for 30−40 min. The sample was then placed under vacuum at 2×10^{-2} Torr for 3−4 h to remove water from the NaCl surface. As a result, a thin polycrystalline NaCl film was formed at the quartz surface.

He (99.995%) was used as the carrier gas and was passed through NaOH and P_2O_5 traps to remove water vapor before entering the flow system. Neither oxygen nor hydrogen atoms were detected in the He discharge by the EPR method; their concentration was less than 5×10^{10} molecule/cm^3.

Results

Figure 3 presents examples of the kinetic decay curves of HO_2. Each point is the average of 3−5 measurements. The data in Figure 3a were obtained by the MIESR method with an initial HO_2 concentration of 4×10^{10} molecule/cm^3. The curves in Figure 3b were obtained by HO_2 titration while recording the EPR signal of the OH radicals in the gas phase at $[HO_2]_0 = 5 \times 10^{11}$ molecule/cm^3. Figure 3 shows that the radical uptake follows first-order kinetics:

$$[HO_2] = [HO_2]_0 \exp(-kt) \qquad (1)$$

where k is the effective rate constant for the heterogeneous HO_2 reaction that occurs at the insert surface.

In earlier work,[9,15] we demonstrated that the formula for additivity of kinetic resistances is valid with high accuracy for

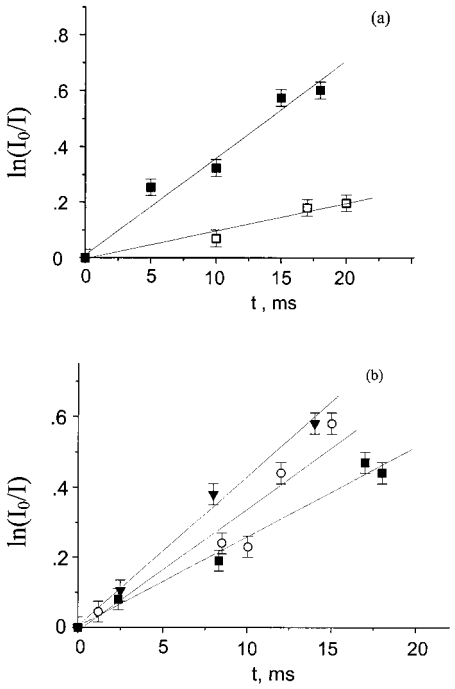

Figure 3. HO_2 heterogeneous loss on NaCl surfaces: Panel (a) $[HO_2] = 4 \times 10^{10}$ molecule/cm^3; □, 345 K and ■, 295 K. Panel (b) $[HO_2] = 5 \times 10^{11}$ molecule/cm^3; ■, 295 K; ○, 270 K; and ▼ −244 K.

laminar flow conditions in the coaxial reactor:

$$1/k = 1/k_{kin} + 1/k_{dif} \qquad (2)$$

The rate constants for the kinetics- and diffusion-controlled reaction k_{kin} and k_{dif} are determined by the equations

$$k_{kin} = 2\gamma/(2-\gamma) \times q/(1-q^2) \times c/2R \qquad (3)$$

$$k_{dif} = K(q)D/R^2 \qquad (4)$$

where c is the average HO_2 thermal velocity, q is the ratio of the insert radius r to the cylinder radius R, $K(q)$ is the dimensionless rate constant for diffusion (which is independent of the gas flow velocity[9,16]), and D is the diffusion coefficient. In our experiments, $K(q = 0.165) = 1.8$ at $[HO_2] = 4 \times 10^{10}$ molecule/cm^3 and $K(q = 0.125) = 1.45$[9,16] at $[HO_2] = 5 \times 10^{11}$ molecule/cm^3.

The diffusion coefficients of HO_2 in He and O_2 were estimated in our earlier work:[9] we used $D_{HO2-He} = 440$ cm^2/s and $D_{HO2-O2} = 116$ cm^2/s at 1 Torr and a temperature dependence given by $D \sim T^{1.75}$.

Table 1 presents the results. The table includes the measured values of the effective rate constant k for the HO_2 decays on the moveable rod, the calculated diffusion-controlled (eq 4) and kinetic-controlled (eq 2) rate constants, and the estimated γ values (eq 3). All of these values remain constant with time for at least 30 min. Table 1a shows that the rate constant for the diffusion-controlled reaction k_{dif} at $[HO_2] = 4 \times 10^{10}$ molecule/cm^3 is much larger than the measured k value. Therefore, in this case, the heterogeneous reaction of HO_2 with NaCl is not controlled by diffusion. Measurements at $[HO_2] = 5 \times 10^{11}$ molecule/cm^3 were carried out under less favorable conditions: in this case, the diffusion correction at 243 K causes a nearly 2-fold change in the γ value.

Figure 4 presents an Arrhenius plot of the γ values measured in this work, as well as our previously reported value measured with $[HO_2] = 4 \times 10^9$ molecule/cm^3 at 295 K[9] (note that in

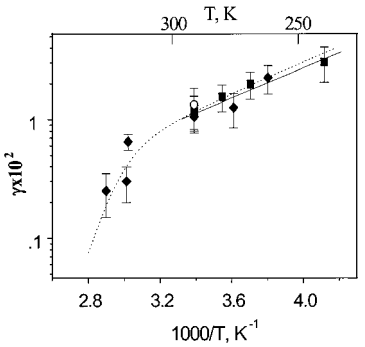

Figure 4. Comparison of experimental results and modeling with the Eley−Rideal mechanism: Experiments: ○, $[HO_2] = 4 \times 10^9$ molecule/cm^3;[9] ◆, $[HO_2] = 4 \times 10^{10}$ molecule/cm^3; and ■ − $[HO_2] = 5 \times 10^{11}$ molecule/cm^3. Solid line: simulation of the experimental results at 240−300 K using an Arrhenius expression. Dashed line: Eley−Rideal modeling using the following parameters: $f_1 = 0.2$, $k_{ads} = c/4$; $A_{1d} = kT/h$, $\Delta H_{ads1} = 20$ kcal/mol; $A_{1r} = 3 \times 10^{-15}$ cm^3/s; $E_1 = -3$ kcal/mol, $Z = 6.4 \times 10^{14}$ molecule/cm^2.

TABLE 1: Rate Constants for the Heterogeneous Uptake of HO_2 on NaCl

(a) $[HO_2] = 4 \times 10^{10}$ molecule/cm^3, $p = 1$ Torr, He:O_2 = 3.86:1, $q = 0.165$, $K(q{=}0.165) = 1.80$.[16]

T, K	k, s^{-1}	k_{dif}, s^{-1}	k_{kin}, s^{-1}	$\gamma \times 100$
345	9.8	500.2	10.0	0.26 ± 0.05
332	11.4	467.7	11.7	0.31 ± 0.05
331	22.2	465.23	23.31	0.62 ± 0.05
295	35.7	380.25	39.40	1.16 ± 0.22
277	39.7	340.63	44.93	1.31 ± 0.24
263	62.15	310.94	77.68	2.31 ± 034

(b) $[HO_2] \sim 5 \times 10^{11}$ molecule/cm^3, $p = 2.3$ Torr, He:O_2 = 5.45:1, $q = 0.125$, $K(q = 0.125) = 1.45$.[9,16]

T, K	k, s^{-1}	k_{dif}, s^{-1}	k_{kin}, s^{-1}	$\gamma \times 100$
295	25.5	144.1	30.96	1.17 ± 0.08
282	30.8	133.1	40.1	1.55 ± 0.13
270	35.7	123.4	50.23	1.98 ± 0.18
243	42.9	102.6	73.72	3.04 ± 0.26

our previous report there was an error in the calculations on passing from the third to the fourth line in Table 4; Figure 4 presents the correct γ value, 1.33×10^{-2}, instead of $\gamma = 1.65 \times 10^{-2}$).

At 243−300 K, all of the results are independent of the initial HO_2 concentration and can be given by the following equation (solid line in Figure 4):

$$\gamma = (5.66 \pm 3.62) \times 10^{-5} \exp[(1560 \pm 140)/T] \quad (5)$$

However, the γ value sharply decreases at 331−335 K with $[HO_2] = 4 \times 10^{10}$ molecule/cm^3 (dashed line in Figure 4).

Discussion

Under our experimental conditions, the consumption of the HO_2 radicals by their self-reaction in the gas-phase occurs much more slowly than their heterogeneous uptake. The maximum rate of the homogeneous HO_2 consumption is 1.6 s^{-1} at 243 K and $[HO_2] = 5 \times 10^{11}$ molecule/cm^3, whereas the rate of the heterogeneous reaction under the same conditions is 43 s^{-1}.

In principle, the heterogeneous uptake of HO_2 radicals by NaCl could be a source of chlorine, as in the following reaction:

$$HO_2 + NaCl = NaOH + {}^1/_2(Cl_2 + O_2) \qquad \Delta H = -6 \text{ kcal/mol} \quad (R1)$$

Reaction R1 is not elementary and may involve the following steps:

$$HO_2 + NaCl \rightarrow NaOH + ClO(ads)$$

$$ClO(ads) + ClO(ads) \rightarrow Cl_2 + O_2$$

The first step is endothermic by 18 kcal/mol if one assumes that the ClO radicals are liberated into the gas phase. If, however, the enthalpy of adsorption of ClO on NaCl is higher than 18 kcal/mol, then the first reaction is exothermic. This appears unlikely, although in some earlier work by Carlier et al.[18] halogen oxide radicals were found to be present in the heterogeneous reaction of hydrogen peroxide with KCl and KBr at $T \geq 200$ °C.

On the other hand, comparison of the coefficient of HO_2 uptake on NaCl (eq 5) with our previous data[14] for NH_4NO_3 at $[HO_2] = 5 \times 10^{11}$ molecule/cm^3

$$\gamma_{HO2}^{NH4NO3} = (5.4 \pm 0.4) \times 10^{-5} \exp[(1540 \pm 200)/T]$$

shows that the two uptake coefficients are practically identical in the temperature range of 243−300 K, although the chemical uptake of the HO_2 radicals does not involve halogen oxides in the latter case. Therefore, we believe that reaction R1 is unlikely to take place below room temperature, and radical uptake most likely occurs largely via surface recombination (disproportionation) for both salts:

$$HO_2(g) + NaCl(s) = {}^1/_2(H_2O_2 + O_2)(g) + NaCl(s) \quad (R2)$$

Reaction (R2) is not elementary, and can occur via either the Eley−Rideal (ER) and Langmuir−Hinshelwood (LH) mechanisms.[19] Both schemes are discussed below. In the ER scheme (reactions R5−R7), the HO_2−NaCl complexes are marked with an asterisk to distinguish them from the less stable HO_2−NaCl complexes involved in the LH mechanism:[19]

$$HO_2(g) + NaCl(s) \rightarrow HO_2{-}NaCl(s)^* \qquad k_{ads} \quad (R5)$$

$$HO_2{-}NaCl(s)^* \rightarrow HO_2(g) + NaCl(s) \qquad k_{1d} \quad (R6)$$

$$HO_2(g) + HO_2{-}NaCl(s)^* \rightarrow \text{products} \qquad k_{1r} \quad (R7)$$

The LH mechanism is described instead by reactions R8−R10:

$$HO_2(g) + NaCl(s) \rightarrow HO_2{-}NaCl(s) \qquad k_{ads} \quad (R8)$$

$$HO_2{-}NaCl(s) \rightarrow HO_2(g) + NaCl(s) \qquad k_{2d} \quad (R9)$$

$$2HO_2{-}NaCl(s) \rightarrow \text{products} \qquad k_{2r} \quad (R10)$$

Adsorption via reactions R5 and R8 occurs at specific sites, and reactions R7 and R10 result either in the liberation of the surface site or in the adsorption of the reaction product on the same site. The model involving reactions R5−R10 is rather simple and ignores the possibility of multilayer adsorption of HO_2 radicals on NaCl.

Our experimental results indicate that the products of reactions R7 and R10 do not inhibit radical uptake, because the rate of HO_2 uptake does not change during an exposure time of at least 30 min.

The kinetics of the change in the surface coverage with HO_2−NaCl* and HO_2−NaCl complexes can be described by eqs 6 and 7, respectively:

$$f_1SZ\,(d\Theta_1/dt) = (k_{ads}[HO_2](1 - \theta_1 - \theta_2) - k_{1d}\theta_1 Z - k_{1r}[HO_2]\,\theta_1 Z)f_1 S \quad (6)$$

$$f_2SZ\,(d\Theta_2/dt) = (k_{ads}[HO_2](1 - \theta_1 - \theta_2) - k_{2d}\theta_2 Z - 2k_{2r}(\theta_2 Z)^2)f_2 S \quad (7)$$

where S is the area of the rod surface inserted into the reactor, f_1 and f_2 are the average fractions of the NaCl sites that favor reactions R7 and R10, respectively, $Z = 6.4 \times 10^{14}$ molecule/cm^2 [20] is the surface density of the Na^+Cl^- ionic pairs, θ_1 and θ_2 are the surface coverages with strongly and weakly bonded adsorbed radicals, respectively, $k_{ads} = \alpha c/4$ is the adsorption rate constant, set equal for both mechanisms, c is the average thermal velocity of the radicals, α is the accommodation coefficient, which was further set equal to unity, and k_{1d} and k_{2d} are the desorption rate constants for HO_2−NaCl* and HO_2−NaCl, which in turn can be expressed in the form $(kT/h)\exp(-\Delta H_{ads}/RT)$, where ΔH_{ads} is the heat of adsorption and k and h are the Boltzmann and Planck constants, respectively. The preexponents of the desorption rate constants were set equal to (kT/h) for both complexes, whereas the heats of adsorption ΔH_{ads1} and ΔH_{ads2} are different ($\Delta H_{ads1} > \Delta H_{ads2}$). The f_1 value was set equal to the average fraction of the NaCl sites occupied by the defects at the NaCl surface; that is, $f_1 = 0.2$.[21] Hence, $f_2 = (1 - f_1) = 0.8$ has no defect sites. If so, the f_1 fraction should have a higher energy of adsorption and should form chemisorbed surface complexes. However, the f_2 fraction with a low energy of adsorption consists of physisorbed complexes. We found this to be the case; that is, $\Delta H_{ads1} > \Delta H_{ads2}$ (see Table 2).

The rate constants k_{1r} and k_{2r} can be represented as Arrhenius expressions $k_{1r} = A_{1r}\exp(-E_1/RT)$ and $k_{2r} = A_{2r}\exp(-E_2/RT)$. The uptake of HO_2 occurs under steady-state conditions and the coverage θ_1 and θ_2 are independent of time

$$d\theta_1/dt = d\theta_2/dt = 0 \quad (8)$$

The characteristic time of the establishment of the steady-state radical uptake is shorter than adsorption duration $\tau = 4S/cV \approx 10^{-3}$ s (S/V is the ratio of the insert surface to the volume of the reactor containing this insert).

In accordance with eqs 6−8, the θ_1 and θ_2 values are determined by the formulas:

$$\theta_1 = d(1 - \theta_2) \quad (9)$$

$$\theta_2 = \frac{-(k_{2d}Z + k_{1r}[HO_2] - dk_{1r}[HO_2]) + \sqrt{J}}{4k_{2r}Z^2} \quad (10)$$

where the d and J parameters are related to the rate constants and the HO_2 concentration by the equations

$$d = \frac{k_{ads}[HO_2]}{k_{ads}[HO_2] + k_{1r}Z[HO_2] + k_{1d}Z} \quad (11)$$

$$J = (k_{2d}Z + k_{ads}[HO_2] - k_{ads}[HO_2]d)^2 + 8k_{2r}Z^2(k_{ads}[HO_2] - k_{ads}[HO_2]d) \quad (12)$$

In accordance with reactions R5−R10 and eqs 6−10, the rate of HO_2 uptake from the volume to the NaCl surface is described by the equation

$$V\frac{d[HO_2]}{dt} = (-2f_1k_{1r}[HO_2]\theta_1 Z - 2f_2k_{2r}(\theta_2 Z)^2)S \quad (13)$$

The probability of the heterogeneous decay of the HO_2 radicals is determined from eqs 13 and 14:

$$V\frac{d[HO_2]}{dt} = -\gamma k_{ads}[HO_2]S \quad (14)$$

In this case

$$\gamma = \frac{2f_2k_{2r}(\theta_2 Z)^2}{k_{ads}[HO_2]} + \frac{2f_1k_{1r}(1 - \theta_2)Z}{k_{ads}} \times d \quad (15)$$

The θ_1 and θ_2 values are given by formulas 9−12.

When the heterogeneous radical uptake is described only by the ER scheme (that is, $\theta_2 = 0$), the heterogeneous reaction probability may be represented by a much simpler equation:

$$\gamma = \frac{2f_1(k_{1r}Z/k_{ads})}{1 + (k_{1r}Z/k_{ads}) + (k_{1d}Z/k_{ads}[HO_2])} \quad (16)$$

We will next analyze whether our experimental results may be described by the ER mechanism involving reasonable parameters. Equation 16 suggests that the γ value depends on the HO_2 concentration when $[HO_2] < k_{1d}Z/k_{ads}$. Below 295 K, the heterogeneous uptake probability is independent of the HO_2 concentrations for $[HO_2] = 4 \times 10^9 - 5 \times 10^{11}$ molecule/cm^3, as shown in Figure 4. Therefore, we may assume that

$$k_{1d}Z/k_{ads}[HO_2] \ll 1 + k_{1r}Z/k_{ads} \quad (17)$$

at $T \le 295$ K for the minimum HO_2 concentration of 4×10^9 molecule/cm^3.

At the same time, the inequality

$$k_{1r}Z/k_{ads} \le 1 \quad (18)$$

should hold within the same temperature range. Otherwise, the γ value would be equal to $2f_1 \approx 0.4$, which contradicts the experimental results both in terms of the absolute value and the temperature dependence of γ. The comparison of eqs 17 and 18 shows that the inequality

$$k_{1d}Z/k_{ads}[HO_2] \ll 1 \quad (19)$$

should apply to the process within the framework of the ER mechanism. In this case, eq 16 may be simplified to

$$\gamma = 2f_1\,(k_{1r}Z/k_{ads}) \quad (20)$$

Taking into account that the maximum value of γ (243 K) $= 3 \times 10^{-2}$ and $2f_1 = 0.4$, inequality 18 is fulfilled because

$$k_{1r}Z/k_{ads} = \gamma/2f_1 = 7.5 \times 10^{-2} \ll 1$$

Using the minimum value $[HO_2] = 4 \times 10^9$ molecule/cm^3 at

TABLE 2: Parameters of the Combined Eley−Rideal (ER) and Langmuir−Hinshelwood (LH) Model

kinetic mechanism	$\Delta H_{ads1,2}$, kcal/mol	A_{1r}, cm^3/s	A_{2r}, cm^2/s	$E_{1,2}$, cal/mol
1. ER	>18.5	1.1×10^{-13}		-750 ± 300
2. LH	9.2 ± 0.5		4×10^{-4}	500 ± 200

295 K, one can easily see that inequality 19 is true for $\Delta H_{ads1} > 19$ kcal/mol, where ΔH_{ads1} is the heat of adsorption for the ER mechanism.

Comparing eq 20 and the experimental dependence

$$\gamma = (5.66 \pm 3.62) \times 10^{-5} \exp(1560 \pm 140/T) \qquad (5)$$

and using $f_1 = 0.2$ and $k_{ads} = 10^4$ cm/s at 245−295 K, we estimate $E_1 = -3100$ cal/mole and $A_1 = 2.5 \times 10^{-15}$ cm^3/s.

Figure 4 presents the experimental γ values for $[HO_2] = 4 \times 10^{10}$ and 5×10^{11} molecule/cm^3 and the theoretical curve of the probability for the heterogeneous uptake of HO_2 (the dashed line) calculated within the framework of the ER mechanism using the parameters $f_1 = 0.2$, $k_{ads} = c/4$, $E_1 = -3$ kcal/mol, $A_{1r} = 3 \times 10^{-15}$ cm^3/s, $\Delta H_{ads1} = 20$ kcal/mol, and $A_{1d} = kT/h$. The theoretical description of $\gamma(T, [HO_2])$ presented in Figure 4 (dashed line) was obtained using six parameters, three of which (f_1, A_{1d}, k_{ads}) were set by us and the remainder being determined by comparing eq 16 with the experimental data. Equation 16 is more sensitive to the A_{1r} and E_1 values. For $[HO_2] = 4 \times 10^{10}$ molecule/cm^3, desorption occurs at high temperatures. Although the theoretical curve $\gamma(T, [HO_2])$ presented in Figure 4 as the dashed line provides a good description of the experiment, the required rate constants for the collision recombination (R7) $A_1 = 3 \times 10^{-15}$ cm^3/s and $E_1 = -3$ kcal/mol seem doubtful, especially in comparison with the parameters of the analogous gas-phase reaction

$$HO_2 + HO_2 \rightarrow H_2O_2 + O_2 \qquad (R11)$$

$$k_{11} = 2.3 \times 10^{-13} \exp(1200/RT) \text{ cm}^3/\text{s}$$ [22]

The preexponential factor for the reaction rate constant for the heterogeneous process (R7) is 2 orders of magnitude smaller than that for the gas-phase reaction (R11); furthermore, the negative activation energy for the heterogeneous reaction is 2.6 times larger than that for the corresponding homogeneous reaction. The temperature dependence with the apparent negative activation energy suggests that both reactions R7 and R11 involve complex formation. However, the difference in the Arrhenius parameters is striking.

Taking this into account, we consider the observed experimental dependence $\gamma(T, [HO_2])$ in terms of both mechanisms. In this case, we set the parameters $f_1 = 0.2$, $f_2 = 0.8$, $k_{ads} = c/4$, and $A_{1d} = A_{2d} = kT/h$ and choose the ΔH_{ads1}, ΔH_{ads2}, A_{1r}, A_{2r}, E_{1r}, and E_{2r} values to get the best coincidence between the theoretical and experimental γ values. Figure 5 presents the experimental and theoretical γ values calculated by equations 9−12 and 15 at the parameters given in Table 2.

The rate constant for the reactions of the adsorbed complexes HO_2−NaCl* (A_{1r}, E_1) and HO_2− NaCl (A_{2r}, E_2) chosen in Table 2 seem quite reasonable. The negative activation energy of reaction R7 suggests that this reaction also involves complex formation as the analogous gas-phase reaction. The A_{2r} and E_2 values indicate that surface diffusion can limit the process.

Note that other reasonable sets of initial parameters may also be found within the framework of both mechanisms. The above parameters correspond to the minimum heats of adsorption $\Delta H_{ads1,2}$, for which the k_{1r} and k_{2r} rate constants seem the most reasonable. For example, the experimental data may satisfactorily be described at $\Delta H_{ads1} > 20$ kcal/mol and $\Delta H_{ads2} = 13-14$ kcal/mole. However, the preexponential factor A_{2r} corresponding to these values is much less than usual. Figures 4 and 5 show that additional experiments should be performed at high temperatures (300−450 K) within a wide concentration range,

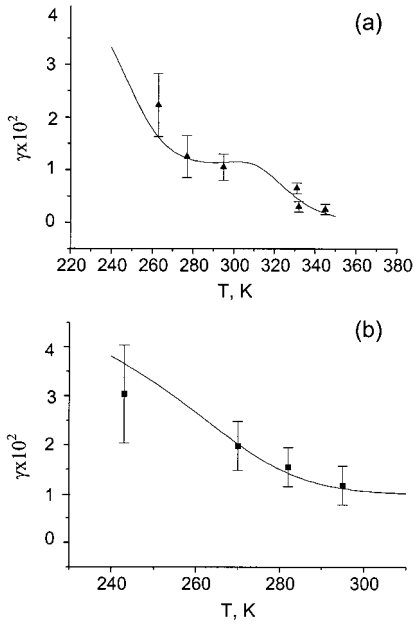

Figure 5. Comparison of experimental results and modeling with the combined Eley−Rideal/Langmuir−Hinshelwood mechanism: Panel (a) ▲, $[HO_2] = 4 \times 10^{10}$ molecule/cm^3. Panel (b) ■, $[HO_2] = 5 \times 10^{11}$ molecule/cm^3. Solid line in panels a and b are the combined Eley−Rideal/Langmuir−Hinshelwood modeling with parameters taken from Table 2.

TABLE 3: Influence of Water Vapor on the HO_2 Uptake Probability

	$[H_2O] = 0$		$[H_2O] = 3 \times 10^{15}$ molecule/cm^3	
T, K	$100 \times \gamma_{exp}$	$100 \times \gamma_{theory}$	$100 \times \gamma_{exp}$	$100 \times \gamma_{theory}$
243	3.04 ± 0.26	3.6	2.39 ± 0.21	2.91
270	1.98 ± 0.18	2.02	1.35 ± 0.18	1.85
295	1.17 ± 0.08	1.11	1.02 ± 0.08	1.1

that is, primarily under conditions of a significant change in the coverage of the surface active sites, to elucidate the final reaction mechanism.

Using the parameters chosen above, we calculate that for $[HO_2]=5 \times 10^{11}$ molecule/cm^3 a sharp decrease in the γ value should take place for $T \geq 380$ K. We plan to conduct additional experiments to test this prediction.

The Effect of Water Vapor. The addition of water vapor into the reactor (into the side inlet, that is, the farthest to the ESR cavity) causes a decrease in the probability of radical uptake, which most likely suggests the absence of a chemical reaction of the radicals with the salt. The inhibition by water vapor may be a consequence of water adsorption on NaCl resulting in a decrease in the number of the free sites available for radical adsorption. Table 3 presents the results of studying the effect of water vapor on the γ values.

Measurements were conducted with $[HO_2] = 5 \times 10^{11}$ molecule/cm^3, $[H_2O] = 0$, and $[H_2O] = 3 \times 10^{15}$ molecule/cm^3. The calculations (γ_{theor}) were performed within the combined ER−LH model using the parameters given in Table 2. The γ_{theor} values were calculated in the presence of water vapor with due regard to water adsorption and desorption:

$$H_2O + NaCl \rightarrow H_2O\text{−}NaCl \qquad k_{adsH_2O} \qquad (R12)$$

$$H_2O\text{−}NaCl \rightarrow H_2O + NaCl \qquad k_{dH_2O} \qquad (R13)$$

The parameters of the rate constants for the reactions R12 and R13 were taken from Barraclough and Hall[23] and from

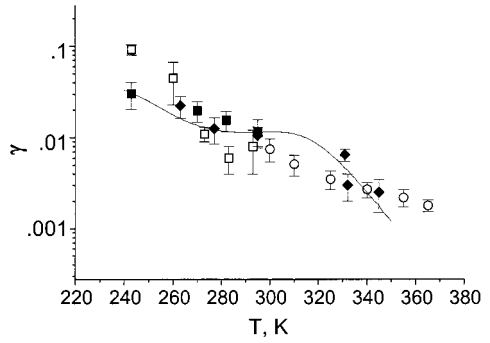

Figure 6. Comparison of experimental results with the combined Eley−Rideal/Langmuir−Hinshelwood modeling mechanism. Experiments: ○, Antsupov;[7] □, Gratpanche et al.;[8] ◆, present work with $[HO_2]$ 4×10^{10} molecule/cm^3; ■, present work with $[HO_2]$ 5×10^{11} molecule/cm^3. Solid line: combined Eley−Rideal/Langmuir−Hinshelwood modeling with parameters taken from Table 2 and using $[HO_2] = 4 \times 10^{10}$ molecule/cm^3.

Vorontzova et al.[24] The heat of physical adsorption of H_2O on NaCl was set equal to 10.5 kcal/mol.[23,24] Using the data on H_2O adsorption [23] at 295 K, we estimated the concentration $[H_2O]_{th} = k_{dH_2O}Z/k_{adsH_2O}$, at which the surface coverage with water is $^1/_2$. The experimental value of $[H_2O]_{th}$ is 1.2×10^{17} molecule/cm^3. Using $Z = 6.4 \times 10^{14}$ molecule/cm^2 [20] and $k_{adsH_2O} = 10^4$ s^{-1} at 295 K, we obtain the temperature dependence of k_{dH_2O} at 243−295 K:

$$k_{dH_2O} = 1.31 \times 10^{14} \exp(-10500/RT)\ \mathrm{s}^{-1}$$

As Table 3 shows, the combined model describes very well the effect of water vapor on the probability of HO_2 uptake. The strongest effect of water vapor on the γ value is observed at low temperatures. The relative decrease in the γ_{exp} value is 21% upon addition of water vapor (3×10^{15} molecule/cm^3), whereas the calculated decrease in the γ_{theor} value in this case is 19%.

Comparison with Previous Results. The temperature dependence of the probability of the heterogeneous uptake of HO_2 on NaCl was studied by Antsupov[7] and by Gratpanche et al.[8] Figure 6 presents the results of these studies as well as the results of our measurements.

Gratpanche et al.[8] observed higher γ values at low temperatures; note, however, that these authors employed a rather large HO_2 concentration ($\sim 5 \times 10^{12}$ molecule/cm^3). The rate of the homogeneous uptake ($HO_2 + HO_2$) in this case was 10−15% of the overall rate of HO_2 decay, and a more accurate consideration of diffusion is probably required in the presence of the second-order gas-phase reaction. Our data agrees well with the results of Antsupov,[7] despite the fact that he used a complex HO_2 source (O_2 discharge + alcohol), which may contain high concentrations of water and other substances adsorbed at the salt surface. According to our estimation, $[HO_2] \sim 10^{11}$ molecule/cm^3 in these experiments.[7] On the other hand, Antsupov did not provide information about $[H_2O]$ and [RH] in his experiments. Nevertheless, we believe that the influence of water vapor is more significant at lower temperatures. Furthermore, oxygen-containing species such as aldehydes, probably present in his system, most likely increased the uptake coefficient compensating for the influence of water. Figure 6 also depicts the theoretical curve calculated within the framework of the model involving both mechanisms using our present results for 4×10^{10} molecule/cm^3. Our parameters for the elementary steps for the two types of adsorption sites seem quite reasonable, although a more accurate determination requires further studies. Figure 6 shows that the theoretical curve satisfactorily describes the elementary data for the three studies at relatively high $[HO_2]$.

Atmospheric Implications. Although the reaction products were not directly determined, the data on HO_2 uptake suggest that reaction R1 resulting in chlorine activation is unlikely to take place. The most likely mechanism is similar to that taking place in the gas phase, that is, involving the self-reaction of the HO_2 radical on the substrate surface. We estimate that in the coastal troposphere the rate of the heterogeneous reaction on solid sea salt particles can become comparable to that of the second order gas phase reaction, particularly in the evening, when the concentration of HO_2 radicals decreases. The effective first-order homogeneous and heterogeneous rate constants of the HO_2 self-reaction may be approximately compared using the following expressions and assumptions:

$$K_{hom} = k_{hom}\,[HO_2]$$

$$K_{het} = 0.25 c \gamma_{ER} 4\pi r^2 N$$

where k_{hom} and K_{hom}(s^{-1}) are the second and effective first-order rate constants of homogeneous HO_2 decay. K_{het}(s^{-1}) is the heterogeneous rate constant of HO_2 uptake on sea salt aerosols, $r \approx 1$ μm is the average radius of particles, and $N \approx 10$ cm^{-3} is the aerosol density. γ_{ER} is the Eley−Rideal part of the uptake coefficient. Using the γ_{ER} instead of the overall γ value, we assume that, at a water pressure of about 10 Torr, the f_2 fraction of the surface is almost completely covered with water. The coverage of the nondefective surface fraction f_2 with physically adsorbed water $\theta^{ph}_{H_2O}$ is approximately 0.5 at $[H_2O] = 1.2 \times 10^{17}$ molecule/cm^3, $T = 290$−295 K ($P_{H_2O} = 3.5$ Torr).[23,24] That is, we assume that effectively the f_2 fraction is not efficient for HO_2 uptake on solid NaCl at 3.5 Torr $< P_{H_2O} <$ 13.5 Torr (the deliquescent point). We also assume that the f_1 fraction is always covered with chemisorbed water that forms active sites for radical uptake with a higher energy of adsorption. For example, if the energy of water chemisorption is $E^{ch}_{H_2O} = 25$ kcal/mol, the f_1 fraction of the surface is almost fully covered with water at $[H_2O] \sim 10^5$ molecule/cm^3, $T = 290$ K. If $E^{ch}_{H_2O} = 20$ kcal/mol, then $\theta^{ch}_{H_2O} = 0.5$ at $[H_2O] = 4 \times 10^{10}$ molecule/cm^3, $T = 290$ K. The water impurity in our experimental system was $(2-3) \times 10^{12}$ molecule/cm^3. Therefore, even under "dry" conditions, the active fraction f_1 might be fully covered with chemisorbed water in our experiments. Our calculations show that, at 275−290 K, the K_{het}/K_{hom} ratio may change from 0.1 to 1 when $[HO_2]$ decreases from 3×10^8 to 3×10^6 molecule/cm^3. We plan to conduct additional experiments to test these conclusions more directly.

Acknowledgment. We acknowledge the active participation of A. V. Ivanov and S. D. Il'in in the elaboration and creation of the new experimental technique employed in this work, as well as their help in the initial stage of these experiments. We also thank R. Zellner, S. Ya. Umanskii, and J.-P. Sawerysyn for useful discussions. The research was supported in part by the CRDF Grant RG-135 and was partly carried out in the frame of the "HAMLET" project of the EU Environment and Climate Program.

References and Notes

(1) Gershenzon, Yu. M.; Ermakov, A. N.; Purmal, A. P. *Chem. Phys. Rep.* **2000**, *19*, 3.

(2) Gershenzon, Yu. M.; Purmal, A. P. *Russian Chem. Rev.* **1990**, *59*, 1007.

(3) Spicer, C. W.; Chapman, E. G.; Finlayson-Pitts, B. J.; Plastridge, R. A.; Hubbe, J. M.; Fast, J. D.; Berkowitz, C. M. *Nature* **1998**, *394*, 353.

(4) Singh, H. B.; Gregory, G. L.; Anderson, B.; Browell, E.; Sachse, G. W.; Davis, D. D.; Crawford, J.; Bradshaw, J. D.; Talbot, R.; Blake, D. R.; Thornton, D.; Newell, R.; Merrill, J. *J. Geoph. Res.* **1996**, *101* (D1), 1907.

(5) Finlayson-Pitts, B. J.; Pitts, J. N. *Atmospheric Chemistry: Fundamentals and Experimental Techniques*; John Wiley and Son: New York, 1986.

(6) Woods, D. C.; Chuan, R. L.; Ride, W. I. *Science* **1985**, *230*, 170.

(7) Antsupov, E. V. *Soviet J. Chem. Phys.* **1988**, *7*, 1082.

(8) Gratpanche, F.; Ivanov, A. V.; Devolder, P.; Gershenzon, Yu. M.; Sawerysyn, J.-P. *Proceeding of Eurotrac Symposium 96*; Borell, P. M., Borrell, P., Kelley, K., Cvitas, T., Seiler, W., Eds.; 1996; p 323.

(9) Gershenzon, Yu. M.; Grigorieva, V. M.; Ivanov, A. V.; Remorov, R. G. *Faraday Discuss.* **1995**, *100*, 83.

(10) Nalbandyan, A. B.; Mantashyan, A. A. *Elemental Processes in the Slow Gas-Phase Reactions*; Erevan, 1975; in Russian.

(11) Baas, A. M.; Broida, H. P. *Formation and Trapping of Free Radicals*; Academic Press: New York, 1960.

(12) Il'in, S. D.; Kishkovich, O. P.; Ivanov, A. V.; Remorov, R. G.; Malkhasyan, Rub. T.; Gershenzon, Yu. M.; Nalbandyan, A. B. *Kinet. Catal.* **1995**, *36*, 448.

(13) Gershenzon, Yu. M.; Il'in, C. D.; Kishkovich, O. P.; Malkhasyan Rub, T.; Rozenshtein, V. B. *Kinet. Catal.* **1982**, *23*, 443.

(14) Gershenzon, Yu. M.; Grigorieva, V. M.; Zasypkin, A. Yu.; Ivanov, A. V.; Remorov, R. G.; Aptekar', E. L. *Chem. Phys. Rep.* **1999**, *18*, 79.

(15) Gershenzon, Yu. M.; Grigorieva, V. M.; Zasypkin, A. Yu.; Remorov, R. G. *13th International Symposium on Gas Kinetics*; Dublin, Ireland, 11−16 September; Book of Abstracts, 1994; p 420.

(16) Remorov, R. G.; Grigorieva, V. M.; Ivanov, A. V.; Sawerysyn, J.-P.; Gershenzon, Yu. M. *13th International Symposium on Gas Kinetics*; Dublin, Ireland, 11−16 September; Book of Abstracts, 1994; p 417.

(17) Ivanov, A. V.; Molina, M. J. Private communication.

(18) Carlier, M.; Sahetchian, K.; Sochet, L.-R. *Chem. Phys. Lett.* **1979**, *66*, 557.

(19) Adamson A. W. *Physical Chemistry of Surfaces*, 3rd ed.; Wiley: New York, 1976.

(20) Kittel C. *Introduction to Solid State Physics*, 6th ed.; Willey: New York, 1986.

(21) Dai, D.; Ewing, C. E. *J. Phys. Chem.* **1993**, *98*, 5050.

(22) DeMore, W. B.; Sander, S. P.; Golden, D. M.; Hampson, R. F.; Kurylo, M. J.; Howard, C. J.; Ravishankara, A. R.; Kolb, C. E.; Molina, M. J. *Chemical Kinetics and Photochemical Data for Use in Stratospheric Modeling*; JPL Publication 97-4; NASA, JPL, 1997.

(23) Barraclough, P. B.; Hall, P. B. *Surf. Sci.* **1974**, *46*, 393.

(24) Vorontzsova, I. K.; Abronin, I. A.; Miheikin, I. D. *Chem. Phys. Rep.* **1999**, *18*, 205.